Analyst

Accepted Manuscript

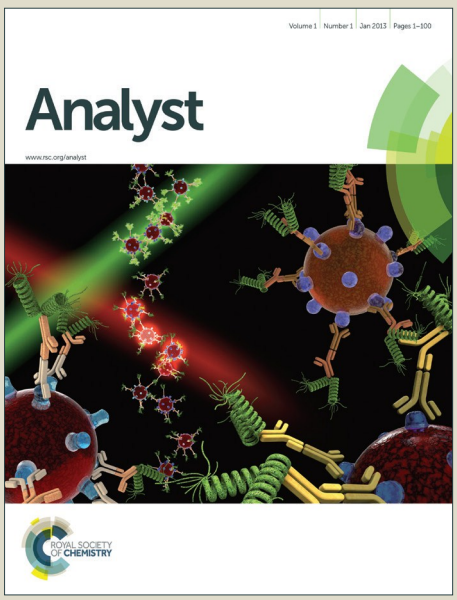

ROYAL SOCIETY OF CHEMISTRY

www.rsc.org/analyst

Manuscript ID AN-ART-03-2015-000483

Title: Synchrotron DUV luminescence micro-imaging to identify and map historical organic coatings on wood

Table of content entry :

Collagen-based materials in historical coatings were characterised and imaged at the sub-micrometer scale using synchrotron DUV luminescence microspectroscopy and spectro-imaging.

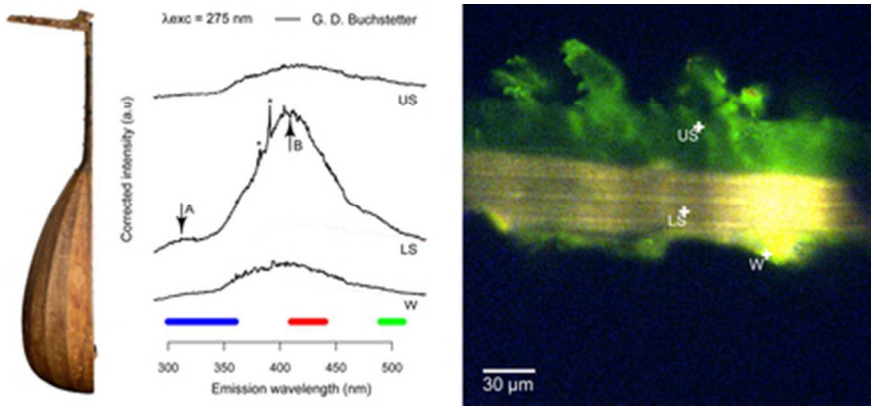

36x16mm (300 x 300 DPI)

Synchrotron DUV luminescence micro-imaging to identify and map historical organic coatings on wood

Jean-Philippe Echard,*[a] Mathieu Thoury,[b,d] Barbara H. Berrie,[c] Tatiana Séverin-Fabiani,[b,d] Alessandra Vichi,[b] Marie Didier,[a] Matthieu Réfrégiers,[d] and Loïc Bertrand[b,d]

Received (in XXX, XXX) Xth XXXXXXXXX 20XX, Accepted Xth XXXXXXXXX 20XX
DOI: 10.1039/b000000x

Deep ultraviolet (DUV) photoluminescence (PL) microimaging is an emerging approach to characterise materials from historical artefacts.[1] Here we further assess the potentials of the method to access a deeper understanding of multi-layered varnishes coating wooden violins and lutes. Cross-section micro samples from important 16th- to 18th-century instruments were investigated using synchrotron PL microimaging and microspectroscopy. Excitation was performed in the DUV and the near ultraviolet (NUV), and emission recorded from the DUV to the visible, at a submicrometric spatial resolution. Intercomparison of microspectroscopy and microimaging was made possible by radiometrically correcting PL spectra both in excitation and emission. Based on an optimised selection of emission and excitation bands, the specific PL features of the organic binding materials allowed a vastly enhanced discrimination between collagen-based sizing layers and oil/resin-based layers compared to epiluminescence microscopy. PL therefore appears as a very promising analytical tool to provide new insights into the diversity of surface coating techniques used by instrument-makers. More generally, our results demonstrate the potential of synchrotron PL for studying complex heterogeneous materials beyond the core application of the technique to Life Sciences.

Introduction

In the context of studies of historical materials and techniques used by artists and artisans, one of the main questions has been to recognise and determine the spatial distribution of organic materials used as binding media, and their reaction products. This is especially applicable in studies of finishing techniques (for furniture and musical instruments) and of painting techniques (for easel paintings and polychrome works).

In particular, the presence of a protein-based sizing agent applied onto wood of musical instruments or furniture, before coating a hydrophobic material to protect the wood, has been discussed.[2-4] For bowed stringed instruments, such as violins, the term “varnish” often names the multi-layered organic coating applied onto the wooden surface of the instrument to finish it, independently of the chemical nature of the layers. Observation of the surface of the instrument under UV illumination has been used to assess the extent of remaining original “varnish" and of retouches on violins.[5-7] Most organic analyses of musical instruments surface coatings were performed on micro scrapings (mostly gas chromatography and IR spectroscopy), however never taking into account the fact that the coatings might be multi-layered systems, and that the analysed matter might come from several layers.[8]

The development of analytical strategies for micro-characterisation of musical instruments surface coatings meets the effort made for a range of heritage materials. In particular, for historical easel paintings, there is a similar problem in determining the nature and spatial distribution of the binding medium in which pigments are admixed in each layer of the stratigraphy, since it may inform on the artists' technique as well as on the material history of the artwork (ageing, chemical alteration, past restorations, etc.). Understanding chemical pathways of binding media is crucial both for conservation and restoration purposes. Modelling from data collected on painting cross-sections is challenging because the pigment concentration is often so elevated that it may be difficult or impossible to collect chemical signatures of the sole binding medium without the contribution of any surrounding pigment particle. In addition, interactions of pigments with the binding medium may hamper collection of chemical signatures of “pure” binding media, naturally aged over centuries. The finishes coating the wood of historical musical instruments, and in particular those of the violin and lute families, rarely contain fillers or pigments (and if they do, in small concentrations). Organic compounds used to coat musical instruments therefore provide interesting systems to study the original composition and century ageing of rather pure historical organic oils, resins and glues. Until the 19th century at least, these multi-layered systems were mostly made of natural organic film-making materials. Cross sections of musical instruments finishes present for each layer a homogenous and continuous surface over several square micrometres or more. They may thus represent most interesting systems to collect reference signatures of binding media, similar in nature and age to historical paintings cross-sections, but without the influence of pigments.

Several analytical approaches have provided inputs to characterise and image the distribution of aged organic compounds in historical cross-sections. Rather than looking for ‘the’ ideal single-method approach, a combination of methods is usually implemented in order to provide minimal modification of the sample, high specificity, high resolution and good imaging characteristics. Surface methods based on secondary ion mass spectrometry were shown efficient to

characterise organic ritual matters on African statuettes and organic binding media in cross-sections of early Netherlandish easel paintings.[9-11] New photonic approaches were developed to overcome limitations in the characterisation of organic materials. Micro-FT-IR spectroscopy and full-field imaging using benchtop or synchrotron sources in various setups have undergone numerous developments.[12-16] ATR µ-FT-IR allows attaining micrometric resolutions at best.[17-19] Multi-technique approaches, for instance combination of FT-IR microspectroscopy, at its limits in terms of spatial resolution, with chromatography on scraping samples (a few tens of µg) allowed identifying chemical signatures of organic substances in cross-sections correlated to their spatial distribution.[20-22] The 3D spatial distribution of two binding materials –a collagen-based glue and a sandarac varnish– has been imaged in a model multilayer coating using the contrast in their respective 2-photon fluorescence emission in two wide spectral ranges.[23]

Photoluminescence (PL) has been used for decades as a phenomenon that enhances contrast in optical microscopy. However, quantitative PL spectroscopy and imaging *per se* have only been scarcely employed to study historical binders, in particular at microscale.[24,25] It recently has been used in combined to surface-enhanced Raman scattering (SERS) for the simultaneous identification of organic colorants and binding media in historic oil paintings.[26]

The scarce use of PL spectroscopy is due notably to the highly complex nature of the response of organic luminophores in the visible under classic excitation ranges (UV/A).[27] This limitation can be overcome by specific fluorescent labelling (tagging) of organic compounds. Tag-based PL provides high-specificity, selectivity and good contrast.[28,29] Important recent approaches involve the tagging of specific proteins in cross-section samples using immunofluorescent microscopy (IFM), ELISA methods and surface- or tip enhanced Raman scattering (SERS, TERS) nanotags complexed to secondary antibodies.[30-33] In the case of historical samples, two main limitations will apply: (1) tagging implies exposing the surface of a sample to irreversible changes, (2) most commercial tags emit in the visible and scattering from semi-transparent media often impairs microscale localisation of the luminescent areas. In addition, SERS requires the application of very high local irradiation doses.

An alternative approach is to collect the autofluorescence contribution from amino acids, photo-oxidation products and protein cross-links, as used in several fields of Life sciences.[34,35] A few microspectrofluorimetry studies have been undertaken on cross-sections using near-UV excitation showing a great potential for the method despite the complex fluorescence response of natural binding media materials.[36,37] Indeed, synchronous scan fluorescence spectroscopy and laser-induced fluorescence (LIF) have been reported to study protein-based materials, suggesting a promising path for advanced characterisation of such materials in art objects.[38-40]

The discrimination of protein-based materials in musical instruments cross-sections using autofluorescence leads to specific difficulties. Animal glues, egg white and yolk are the protein-based film-making materials most frequently encountered.[8] Previous works have shown that both animal glues and egg white have excitation maxima at around 280 and 360 nm.[41] The latter excitation is available on commercial instruments through the 365 nm line of mercury lamps, and is therefore the most commonly used. However, associated luminescence spectra in the visible region have several limitations for accurate discrimination of compounds: (a) they are comparable to emissions obtained from non-protein film-forming materials encountered in musical instruments surface coatings, such as drying oils and natural resins, (b) emissions are broad and unstructured, (c) emissions in the visible will be subject to scattering effects. These limitations are likely to hamper discrimination between oil-/resin-based materials and protein-based materials.[42]

Within this work, we exploit synchrotron radiation to use excitation in the deep and the near ultraviolet (DUV, below 320 nm, and NUV) and collect emission from the DUV up to the visible range. We show that synchrotron DUV luminescence microimaging can profitably be inserted in a sequence of methods to allow (i) mapping, discrimination and characterisation of organic species in multilayer coating cross- and thin-sections; (ii) with minimal damage to the sample, including without the addition of any extraneous compound nor tagging that would modify or contaminate the sample f subsequent analyses; (iii) at the micrometre or sub-micrometre scale, which are the typical known scales of heterogeneity such samples: layers thicknesses of a few micrometres, average distance between two neighbouring pigment particles often le than a micrometre; (iv) with an extended spatial dynamics,[43] here imaging areas of 100×100 µm^2 with micrometric spatial resolution.

The application of this method to four coating systems of 16th- to 18th-century musical instruments is presented to address th potential contribution of the method to the understanding of historical materials and techniques for coating musical instruments.

Methods and materials

Synchrotron luminescence microspectroscopy

The white beam of the DISCO beamline at the SOLEIL synchrotron is monochromatised using an iHR320 monochromator (Jobin-Yvon Horiba, Longjumeau, France) before coupling to the entrance of the Polypheme endstation. Emission spectra were collected using monochromat excitation wavelengths in the 250–300 nm range with a UVB beamsplitter (BTQ-250-320-2503M-UV, CVI Melles Griot).[1,44] Spectra were collected using a -70°C Peltier cooled iDus CC (Andor) of 1024×256 pixels with a 26×26 µm^2 pixel size. All data from Polypheme (Fig. 1) were despiked by applying a running median for pixels whose intensity exceeded a median absolute deviation (MAD) criterion.

Absolute calibration of microspectroscopy data

Spectra were corrected for the source intensity and the beamsplitter reflectance on the excitation path, after determination of the variation of the source intensity as a function of the excitation wavelength using an AXUV photodiode positioned between the monochromator and the entrance port of the microscope.[45]

Spectra were also corrected on the detection chain. The spectral response of the Polypheme microscope was calibrated against the Fluorolog calibrated spectrofluorimeter at Horiba Europe Research Center (Palaiseau, France) in the UV/visible range. Spectra from the latter are corrected from the response of the optical chain of the instrument, the variation as a function of time of the source flux, and the detector response. A homemade luminescent standard was used; polystyrene beads (Sigma Aldrich, ref. 430102) were ground to a powder and pressed to form a 0.8-mm thick pellet. The calibration curve was produced from the ratio between the signal detected on the Polypheme microscope under the experimental conditions used on the samples (excitations at 275 and 340 nm, 40× objective, UVB beamsplitter) and a reference spectrum recorded on the calibrated spectrofluorimeter at each wavelength.

A running median was further applied to the calibration curve (window: 11 abscissa points, i.e. 5.8 nm) to smooth fluctuations from noise. Spectral calibration was performed from 287 nm to 531 nm. Above 531 nm, the luminescent signal of the polystyrene standard is too weak to extract a significant response. Spectra were processed and rendered using self-written procedures within the R statistical computing environment[46] and the SpectroMicro package.

Synchrotron multiband micro-imaging

Here the monochromatised beam was reflected toward the entrance of a modified Zeiss Axio Observer Z1 microscope (Carl Zeiss, Germany), on the Telemos endstation.[47] Images acquired were collected using excitation wavelengths of 275 nm and 340 nm. Sharp short-wave reflecting dichroic beamsplitters (Omega Optical, Brattleboro, USA) – respectively at 300 nm or 400 nm depending on the excitation wavelength – reflect the incident monochromatic light upward through a Zeiss Ultrafluar 40× objective (N.A. 0.6). The emitted light was filtered through emission bandpass filters (Omega Optical, Brattleboro, USA). Two full-field detectors were used to record the images of the multiband cubes presented in this study. Rather than 'multispectral', the term 'multiband' here denotes images collected in a limited number of 15–30 nm spectral bands. A Hamamatsu C9100-02 EM-CCD camera was used in 2×2 binning mode resulting in 500×500 pixels images, with 50 (Buchstetter, Fig. 2a) or 100 (Stradivari, Fig. 2b) accumulations of 10 s acquisitions. The projected pixel size in this configuration was 387 nm. Saturated pixels, due to heterogeneity of dark current response of isolated pixels within the Hamamatsu sensor, were removed using the "remove outliers" tools in imageJ. A Princeton PIXIS 1024B/BUV camera (1024×1024 pixels) was used for the Aman and Maler samples (Figs 3 and 4), with acquisition times optimised to the camera dynamic. The projected pixel size was then 313 nm. Each image collected at Telemos was corrected for dark field. Dark field images were collected for each acquisition duration. Artefactual periodical patterns due to readout noise at very low light levels were corrected on very low-luminescence images using Fourier-transform filtering (Fig. 3c). Images of each multiband cube were registered (translation/rotation) using the ImageJ Template Matching plug-in and cropped. When necessary, the data recorded with the PIXIS camera (Fig. 3 and 4e–h) were corrected for the deviation of the detector linearity as a function of integration time. Stretching procedures were used to rescale the pixel intensity values to allow intercomparisons (2–98% percentile in Figs 2, 3b and 3c), or to allow optimum enhancement of visual contrasts (equalization in Fig. 3a; Gaussian stretch in Fig. 4 h).

Epiluminescence microscopy

Epiluminescence microscopy was performed using a Zeiss Axio Scope.A1 microscope. The incident light produced by the mercury lamp was filtered using a bandpass filter (365 nm, 12 nm FWHM). A sharp dichroic beamsplitter (395 nm) reflected radiation downward through a Zeiss LD Epiplan 20× objective (N.A. 0.40). The emitted light was filtered through an emission longpass filter (cut-on 397 nm). Images were acquired using a Leica DFC 320 camera.

Coatings of historical musical instruments

Our aim was to investigate the benefits of synchrotron-based DUV luminescence and to optimise its use for the study of historical micro-samples. We therefore selected micro-samples from four instruments whose coating systems had been investigated previously using other methods, and shown to be of very distinct stratigraphic compositions. Specifically, two have protein-based lower strata, while the others were shown to have oil-based lower strata (see *below*).

The four samples comprise a diversity of materials (nature, concentration, layer thickness, alteration products) encountered in the stratigraphic structure of coatings on historical instruments.

(a) a 16th-century Bolognese lute by Laux Maler

One of the earliest surviving Italian lutes, made by Laux Maler before 1552 in Bologna (Musée de la musique, Paris, inv. num. E.2005.3.1) was included in this study.[48] Earlier work using light microscopy and Py-GC/MS showed that the coating comprises two strata of distinct compositions applied onto a wood (*Fraxinus* sp.), the lower layer is drying-oil based and the upper one contains both a drying oil and a diterpenic *Pinaceae* resin.[22] The sample was embedded in methacrylate-based Technovit 2000LC resin (Heraeus Kulzer) and its surface was prepared using an ultramicrotome.

(b) two 18th-century German lutes

Two instruments were studied, both from the lute family: a theorbo made by Georg Aman in Augsburg in 1739 and a mandora made by Gabriel Davit Buchstetter in Regensburg in 1746 (Musée de la musique, Paris, respectively inv. num. E.2346 and D.AD.40382).[48] Both coating systems are made of two layers applied onto maple wood (*Acer*). Proteinaceous compounds have been previously identified as the major components of the lower layer of both instruments using SR-μ-FT-IR spectroscopy, and GC-MS amino acids analysis confirmed a collagen-based medium in the case of the Buchstetter sample. Molecular markers of a drying oil and a *Pinaceae* resin have been identified in the upper strata of both coating systems using Py-GC-MS.[49]

Micro samples from each instrument were prepared using a microtome without any prior embedding, thereby producing a

rougher surface, but with the distinct advantage of not introducing any extraneous material that would contaminate the samples.

(c) a 18th-century violin by Antonio Stradivari

A violin made by Antonio Stradivari in Cremona in 1716 was included (the 'Provigny' violin, Musée de la musique, Paris, inv. num. E.1730). Its two-layer coating system was previously characterised using a range of analytical methods.[20] The lower stratum is based on a drying oil, whereas the upper one is a mixture of a drying oil and a *Pinaceae* resin, to which red aluminium-containing lake pigments (probably Mexican cochineal) were incorporated. The unembedded cross-section sample was sectioned to a thickness of 2 µm using ultramicrotomy and then deposited onto a silver-coated low-emissivity microscope slide (MirrIR, Kevley Technologies).

Results and discussion

Specificity of the response from protein-based materials

Aged animal glues and egg white have an excitation band in the DUV with a maximum between 270 and 290 nm leading to emission over 300–500 nm,[39] as also observed in fresh protein-based materials.[44] The DUV excitation available at the synchrotron source resulted being far more effective than the conventional 365 nm of laboratory mercury lamp to discriminate among organic compounds encountered in our historical cross-sections.. The excitation available at DISCO is continuously tunable between 200 and 600 nm.[44,47] Emission spectra were collected for a 275 nm excitation on the Buchstetter and the Stradivari cross-sections in areas considered homogeneous at the scale of a few micrometres, in order to compare the luminescence of both coating systems measured in identical experimental conditions (Fig. 1, left panel).

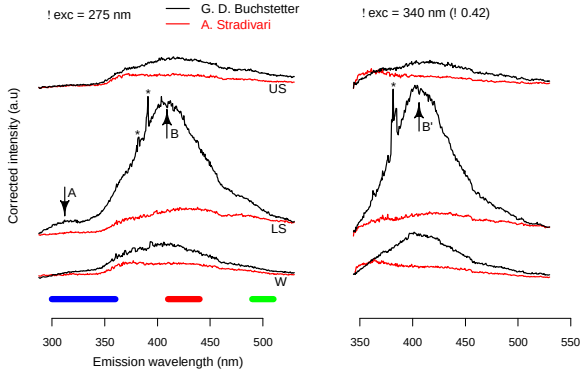

Fig. 1 Corrected emission spectra obtained on 4×4 µm² areas from the wood substrate (W), the lower stratum (LS) and the upper stratum (US) of the cross sections from the Buchstetter (black) and Stradivari (red) instruments on the Polypheme synchrotron setup under 275 nm (left) and 340 nm (right) excitation. Spectra were collected under identical conditions (acquisition time: 300 s, spot size: ca. 1 µm). Samples differ primarily by the photoluminescence of their lower strata (see text for explanation). The blue, green and red segments indicate the bandpasses of the filters used for full-field acquisitions (Fig. 2). Asterisks (*) denote spikes that could not be eliminated through our filtering process, due to the acquisition times. See text for an explanation of A and B.

Emission spectra were also collected using 340 nm excitation in otherwise identical conditions, at the exact same locations on the samples (Fig. 1, right).

The composition of the upper strata of both instruments is known to be made of *Pinaceae* resin admixed with drying oil. The luminescence spectra collected from upper strata of both samples are thus very similar, exhibiting broad overlapping bands with maxima at around 430 nm and possibly around 360–380 nm. The band at around 430 nm is the most intense. These features are unchanged when these materials are excited with a longer wavelength, typically 340 nm, showing that these emissions do not result from an excitation specific to DUV light (Fig. 1). These emission features are associated with the luminescence spectra of aged oil[50] and resin films.[42,51]

The lower stratum of the Stradivari coating, previously characterised as a drying oil, has a luminescence spectrum similar to those of the two upper strata. In contrast, the spectrum from the lower stratum of the Buchstetter sample differs markedly in shape and in intensity. The emission maximum at 409 nm (marked 'B' on Fig. 1) dominates the response of this collagen-based layer. Fibril-forming collagens from various tissues including skin and bovine cartilage exhibit a strong emission in this wavelength domain, attributed to emissions from collagen cross-links.[52,53] In particular, the mature trivalent collagen cross-links residues lysyl and hydroxylysyl pyridinoline are known to luminesce with emission maxima reported between 395 and 405 nm.[54] *In vivo* variations in cross-linking chemistry appear to be more related to type of tissue than type of collagen.[55] The "B" feature can therefore be considered as diagnostic for the presence of aged collagen. The fluorescence properties of such cross-links are strongly dependant of the environment. A further development of this study could thus aim at gaining information on local chemical environment of collagen.

An emission band between 300 and 330 nm occurring on irradiating at 275 nm, appears only in the Buchstetter lower stratum (marked 'A' on Fig. 1). Although this weak residual contribution centred at 312 nm is comparatively less intense than that of the band in the visible range, it stands out as a clear discriminating factor between protein-based and non-protein-based strata. Contributions around 305 nm and at 340–360 nm are common in proteinaceous materials and are attributed to the amino acids tyrosine (Tyr) and tryptophan (Trp) respectively.[56] Collagen molecules do not contain Trp moieties in their triple helical domains and Tyr accounts only for 1.0 % of pure collagen.[38,57] The intensity of the Tyr and Trp contributions to the emission spectrum may have been further weakened by quenching of their luminescence by surrounding polypeptide chains and various functional moieties.[58] In our spectra, contributions from Tyr and Trp therefore appear more intense than would be expected from pure collagen. These signals may be a signature of trace amounts of proteinaceous compounds in addition to collagen. These could easily derive from the manufacturing processes used in the 16th to 18th century that were not aimed at producing highly purified collagen. Indeed, hide and bone glues were obtained by hot water extraction of cattle skins and bones respectively.[59]

Our full spectral correction allows a quantitative comparison of spectra collected using λ_{exc} = 275 and λ_{exc} = 340 nm. The

significantly more intense signal at 340 nm (taking into account the ratio in flux at the sample position: 0.42) is comparable to published data on parchment glue.[39]

Using excitation at both 275 nm and 340 nm allowed a very neat differentiation between the protein and oil/resin-based strata (Fig. 1). Under the 275 nm excitation wavelength, more diagnostic fluorophores are observed, in particular for protein-based materials below 360 nm. In addition, several distinct emission bands above 450 nm are measurable and may be associated to the alteration and ageing of the films.[39]

In addition, more subtle features that stand out of the experimental noise are detected in a region of the Stradivari sample where the wood has not been impregnated by surface coating (Fig. 1, W). The wood substrate emits a weak luminescence, mainly at wavelengths > 400 nm, with at least two distinct contributions, one centred around 410-430 nm and the other in the 500-nm region. In modern wood samples, emission of the para-coumaric and ferulic acids are typically centred at c. 400 and 415 nm, while lignin leads to a broad contribution beyond 380 nm that reaches a maximum around 480 nm and slowly decreases at longer wavelengths.[44,60] In comparison, the luminescence spectrum obtained from wood fibres from the Buchstetter could indicate that they are impregnated with collagen-based glue.

Mapping and quantitative assessment of collagen-based material

The significant contrast of the features in the spectra, even after centuries long ageing of the materials, allowed clear discrimination between surface coating layers using multiband imaging. We produced images from the most characteristic spectral features. The distribution of the protein-based material in the cross-sections is straightforwardly imaged using 275-nm excitation and by selecting regions of the spectra using filters centred at 330, 450, and 550 nm to produce false colour RGB images with a contrast more specific to protein-based materials (Fig. 2).

Fig. 2 shows that the contrast observed with point analysis (c. 4×4 μm^2) is consistent over the whole stratigraphy and individual strata, i.e. thousands of square micrometres. On an ontological aspect, the spatial distribution of the response from the three emission bands validates the notion of 'stratum' with relative internal emission consistency and well-defined boundaries. In particular, the response from the proteinaceous material is concentrated in the Buchstetter lower stratum.

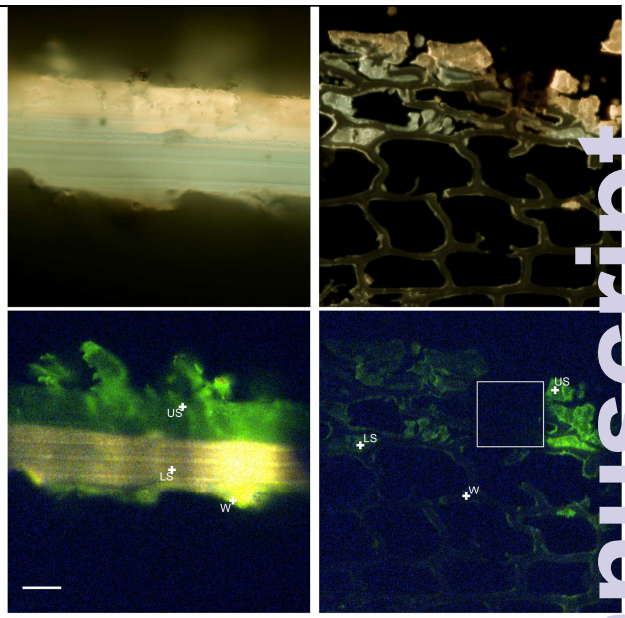

(a) Buchstetter (b) Stradivari

Fig. 2 Visible epiluminescence microscopy (top) and composite RGB images constructed from the synchrotron full-field multiband imag (bottom) of the cross sections of the Buchstetter (a) and Stradivari (b) instruments under 275 nm excitation. Colour designation in a and blue 330 nm, 60 nm FWHM, green 500 nm, 20 nm FWHM, red 425 nm, 30 nm FWHM. To allow intercomparison, in each channel, the lowest value of the 2nd percentile and the highest value of the 98th percentile of the intensity distribution for both images were used as en points for an intensity stretch. Scale bar 30 µm (a and b collected at the same magnification). The white crosses indicate spots where spectra in Figure 1 were collected. The white square in (b) indicates an area previously analysed using SEM-EDX.

Relative luminescence intensities between micro-imaging and microspectroscopy were quantitatively compared. Ratios of specific band intensities are listed in Table 1. The upper stratum of the Buchstetter and the two strata of the Stradivar all oil/resin-based, have similar emission intensity ratios i microspectroscopy. The emission ratios obtained from micro imaging on these same strata are also very similar. It sugges that calculation of emission ratios gives comparable results whether they are obtained from micro-imaging (full-fie imaging) or from micro-spectroscopy (spot analyses). Furthermore, these ratios are all in the range 1.62±15% In contrast, the ratio in intensity between bands centred at 425 nm and 500 nm calculated for the collagen-based lower stratum of the Buchstetter sample is significantly greater (on average 2.5×) than those calculated for the three other strata using either setup.

Our results therefore indicate that the first coat on the wood of the lute made by G.D. Buchstetter was made of a very distinct, collagen-based, material, very probably animal glue. The German instrument-maker applied this size in a coat slightly > 30 µm thick at the sampling spot location. The results of the imaging established that collagen-based binding media can be discriminated from oil/resin-based ones by processing of appropriate bands from multiband data and confirmed that quantitative data intercomparison can be successfully attained despite all setup-related biases.

Table 1 Emission intensity ratios in the 425 nm band (30 nm FWHM) to that in the 500 nm band (20 nm FWHM) from synchrotron microspectroscopy and microimaging data.

		Microspectroscopy	Micro-imaging
Buchstetter	lower stratum	**3.82**	**3.99**
	upper stratum	1.67	1.39
Stradivari	lower stratum	1.42	1.86
	upper stratum	1.44	1.44*

For microspectroscopy data, corrected spectra presented in Fig. 1 were convoluted with the transmittance function of the bandpass filters and the spectral response of the detector, then integrated to obtain corrected intensities. For micro-imaging data, 15×15 pixel areas including the analysed area in microspectroscopy measurements were selected to generate an area similar to the beam size in micro-spectroscopy. The intensity of these pixels was averaged. The micro-imaging setup is not intensity-calibrated in detection but the response of the camera is flat in the 425–500 nm range. A linear correction factor was used to bring the value for the upper stratum of the Stradivari instrument (denoted by *) to the calibrated microspectroscopy value.

Imaging of diagnostic protein-based contributions

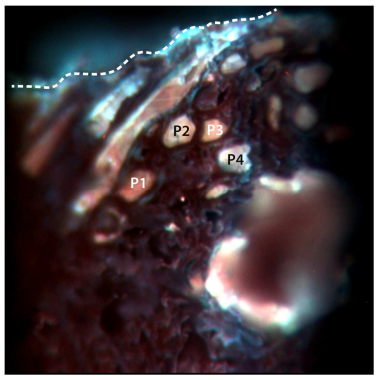

(a) RGB

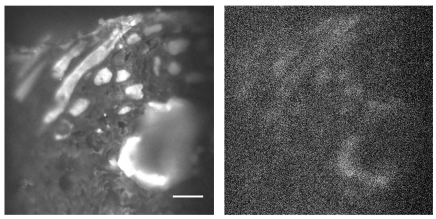

(b) 340 nm (c) 308 nm

Fig. 3 Synchrotron full-field images of the cross-section of the Aman theorbo under 275 nm excitation. Scale bar 20 µm. A protein-based sizing fills the wood pores. Only fragments of the upper stratum remained attached to the sample during the surfacing, which was done without embedding the cross-section. (a) Spatially registered false-colour RGB image of the emission from the sample, with colour designation: blue 425 nm, 30 nm FWHM, green 500 nm, 20 nm FWHM, red 340 nm, 15 nm FWHM. P1–4 are typical wood pores that appear filled with a protein-based compound. Image intensity levels in each channel were adjusted using an equalization stretch (b,c) Images of the location of emission of characteristic bands of tryptophan (a; 340 nm, 15 nm FWHM, 1800 s), and tyrosine (b; 308 nm, 10 nm, 9000 s). Image intensity levels in each channel were adjusted using a 2-98% percentile stretch.

The capabilities of the approach described here were further tested on other samples. In the Aman theorbo, a protein-based compound fills the wood pores, just under coating system (Fig. 3a, P1–4). It is clearly differentiated from the wood cell walls (dark). The blue colour observed in Fig. 3a corresponds to the remnants of a top resin-based coating above the wood surface and the protein-based compound.

Specific chemical imaging can be performed further into th DUV region using narrow-band interference filters in the domains of the weaker bands of the tryptophan and tyrosine amino acids (Fig. 3b and c respectively collected at 340 and 308 nm). Heterogeneities in the signals attributed to collagen cross-links and to Trp in particular can be observed owing to the high signal dynamics of the imaging system. The observed heterogeneity, in a layer usually regarded as homogeneous at this length scale, could be due to the segregation of characteristic luminophores of the coating layers during manufacturing and/or alteration over time. This result shows that specific protein-based materials are potentially selectively imaged and characterised using this straightforward protocol by exploiting tyrosine and tryptophan signatures. In such experimental conditions, noise from the camera and cosmic spikes become significant and it is crucial that they are minimised by using an optimal setup configuration, calibration and data post-treatment.

Practical comparison with conventional epiluminescence microscopy

Mercury lamps providing a 365-nm line are commonly used as near-UV illuminant to examine works of arts and cross-sections with benchtop fluorescence microscopes using an RGB CCD camera to collect images (typical detection channels: red 610 nm, green 530 nm, blue 460 nm; 90 nm FWHM). The capabilities of synchrotron DUV photoluminescence can be further illustrated by comparison with conventional epiluminescence microscopy (Fig. 4).

Taking as an example a cross-section sample from the surface of a lute by Laux Maler (Fig. 4a), several film-forming materials can be evidenced with the mercury lamp illumination. Conventional examination would conclude that a material, appearing lighter in colour, fills most of the wood pores. A film that has a slightly yellower emission can be visualised in the upper part of the wood material, and slightly covering it. It is not straightforward to determine whether there is a distinct boundary between this yellowish material and the one that has a whiter emission and which fills the wood pores. Fragments of the cracked upper stratum, which appear of a very dark red hue under visible illumination, have almost no luminescence under the mercury lamp.

High-resolution synchrotron DUV photoluminescence coupled to multiband detection led to significantly more informative images (Fig. 4e-h). The multiplicity of bands collected provides more capabilities to discriminate materials, based on their luminescence properties. It increases the number of possible 3-band combinations for visualisation using false colour rendering. The signal of the embedding medium (A, Fig. 4e) strongly contrasts with that from the sample, in particular the coat of varnish (*e.g.* B).

The visualisation of the distribution of emission spectra allowed us to discern the extent of penetration of the embedding medium in the sample. This is a challenge, and often not possible, using conventional epiluminescen

conditions (Fig. 4d). The issue of impregnation and contamination from embedding media is always in play during the interpretation of analyses (for instance µFT-IR) on historical organic materials in cross sections. Our methodology simplifies such discrimination, as seen in the case of wood pores impregnated by the embedding medium (*e.g.* C).

Using DUV luminescence imaging provides further information on more localised features. Contrast from compositional variations is enhanced between strata of the coating film that appeared homogenous using the conventional epiluminescence microscope (D,E; Fig. 4f and a).

The secondary walls (F; Fig. 4g and b), appear more luminescent than the compound middle lamella (G), therefore improving the description of the microstructure of the wood cell walls.[61,62] This luminescence from the secondary walls is compatible with that of lignin compounds, with a quite broad emission band, peaking around 340–400 nm when excited in the 240–320 nm range.[60,63] Contrast can also be observed between wood cell walls that exhibit distinctly different luminescence behaviours (H,I; Fig 4h). These results therefore suggest a new path for characterizing and studying microscopic features of organic materials in historical cross sections.

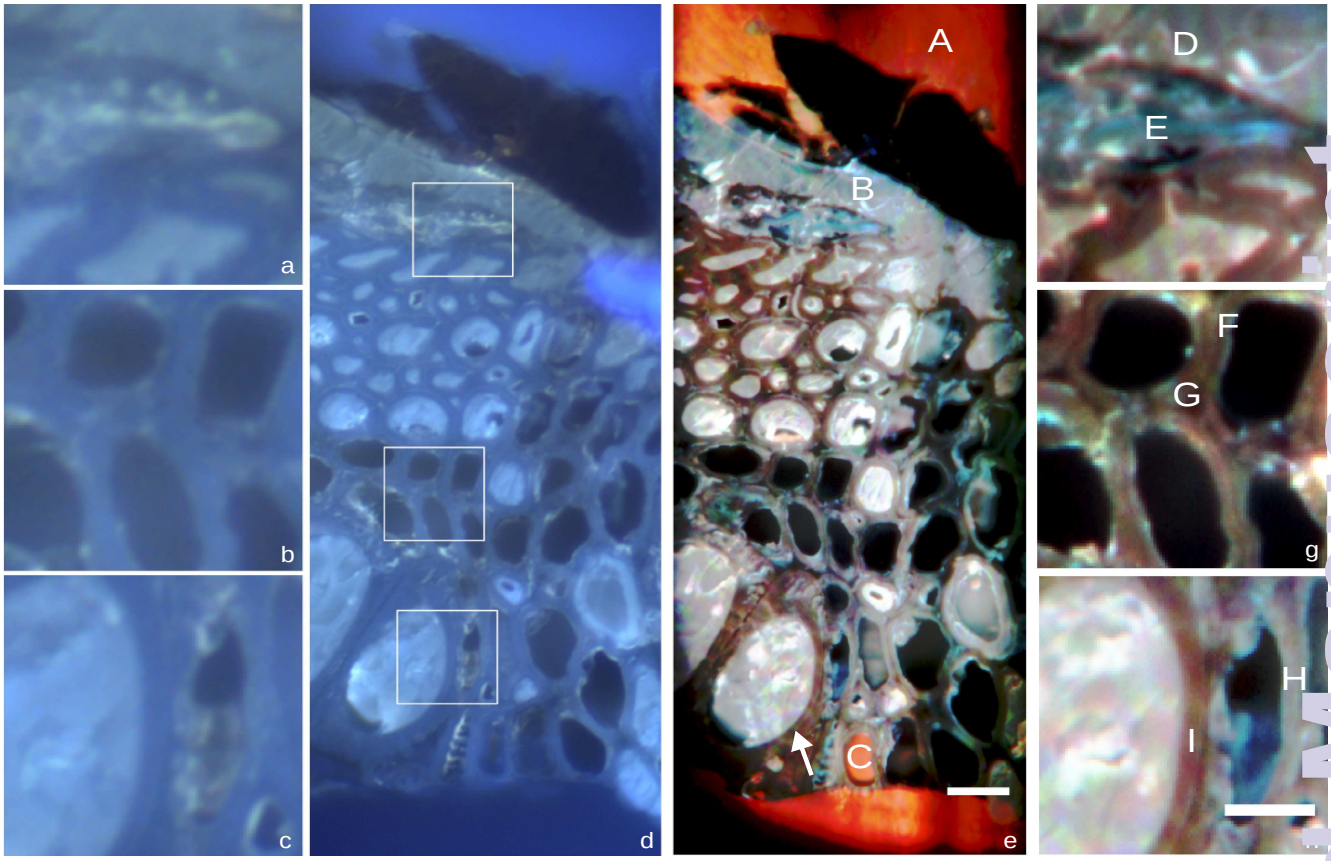

Fig. 4 Comparison between standard epiluminescence and synchrotron full-field multiband imaging on a cross section sample of the Laux Maler surface coating, one of the earliest surviving Italian lutes. (a, b, c) Detailed areas, corresponding to those indicated by the white rectangles in visible epiluminescence light microscopy (d). (d) Visible epiluminescence light microscopy collected with 365-nm mercury excitation. (e) Spatially-registered false-colour RGB 600×600 pixels image constructed from the synchrotron full-field multiband imaging under 275 nm excitation with colour designation: blue 500 nm, 20 nm FWHM, green 465 nm, 30 nm FWHM, red 380 nm, 15 nm FWHM. Image intensity levels in each channel were adjusted using equalisation stretch. Scale bar 40 µm. (f, g, h) Detailed areas, corresponding to those indicated by white rectangles in (d). Scale bar 20 µm. Image intensity levels in each channel were adjusted using a Gaussian stretch. See text for explanation. Local areas designated by letters A–I are described in the text.

On the Stradivari sample, no fluorescence is emitted from a rectangular area in the sample (marked by a white box in Fig 2b). This dark rectangle corresponds to the area of an elemental map previously collected with SEM-EDX. The electron probe has modified the sample namely through degradation of the organic fraction and/or surface carbon deposition, thereby preventing later observation of its luminescence. This illustrates the importance of planning the sequence of analytical techniques performed on each sample, from the least to the most damaging.[64]

High-resolution DUV micro-imaging provides a direct way to identify areas previously altered under an electron beam and possibly other sorts of irradiation such as intense ion or X-ray beam.

Conclusion and perspectives

The results presented here demonstrate the strong assets of synchrotron DUV luminescence analysis over conventional methods in terms of excitation tunability, spatial resolution, multiband imaging:

Tunability. The tunability of the synchrotron beam wavelength allowed, for the first time, the discrimination among organic-based film-forming materials within historical cross-section in the DUV[47,65]. Monochromatic excitation could be adjusted for each system under investigation from the visible to the DUV to optimize the contrast, at the expense of the flux irradiating the sample, which anyhow needed to be kept at moderate values to prevent any radiation-induced effects. No radiation-induced effect was noticed under the conditions used here. The use of tunable excitation conditions is expected to provide an additional powerful contrasting and analytical improvements in characterization of materials.

Resolution. In this work we imaged the distribution of a collagen-based material with 20× the spatial resolution of µ-FT-IR imaging at the diffraction limit.[20,21] DUV excitation combined to a high numerical objective allowed to attain high spatial resolution compare to conventional microscopy or FT-IR microspectroscopy while allowing the analyses of a variety of types of samples. The diversity of samples studied in this work, prepared in many different ways (thin section, cross-section, unembedded ultramicrotomy), demonstrates the wide applicability of the approach for the cultural heritage field. The quality of the surface of the sample is less critical for data quality than for µ-FT-IR spectroscopy in ATR or reflectance mode.[66] Moreover, our approach does not require critical alignment nor contact, which might lead to damage as in evanescent-wave measurements or near-field spectroscopy.

Sub-micrometric spatial resolution combined with spectral selectivity suggest that even heterogeneity within micrometric layers could be imaged in historical organic materials, thus providing key information on preparation, alteration or ageing processes.

Multiband imaging. We have shown that chemical contrast is increased by selecting appropriate bands from the multiband data cubes, here 15 to 30 nm FWHM, centred on the wavelengths of major interest, instead of using a RGB colour camera optimised for real-to-life visualisation. We developed a procedure to obtain quantitative data from the data cubes, which are in good agreement with results obtained using microspectroscopy, while colour images provided by conventional UV-induced luminescence microscopy, using RGB cameras can be misleading for identification of materials.

Our approach provided key information about the surface coatings materials and techniques of 16th–18th-century instrument makers, when it was applied to a series of organic coatings on historical musical instruments: Here we showed that two German 18th-century instruments were first coated with a glue size on the wood, before applying an oil/resin coat of varnish. The only other known example is a French 18th-century instrument.[21] Interestingly, these three instruments were made 'north of the Alps'. In contrast, Antonio Stradivari, celebrated as the finest South-of-the-Alps maker, used a different coating technique: no collagen-based compound was detected using PL spectroscopy and imaging, confirming previous results obtained by IR spectroscopy and chromatographic analyses.[20]

This method could also lead to novel developments in the finer characterization of binding media in easel paintings. The film-making materials used for musical instruments and easel paintings were similar, or even identical until at least the early 19th century. Taking benefit of the high spatial resolution of the technique, further development could (a) exploit the strong influence of pH on the excitation maxima of collagen cross-links to gain information on local chemical environment of collagen, which is known to evolve with (ageing) time, (b) describe the microscale heterogeneity of collagen-based materials to refine identification of the raw materials. Synchrotron DUV/visible photoluminescence analysis may also allow the detection and imaging of colorants, such as gums, resins, dyes and lakes with are otherwise barely detectable in cross-sections otherwise, and often require micro-destructive chromatographic analyses.[67] However, specific issues need to be addressed in the case of easel painting materials. Historical varnishes of musical instruments contain mostly organic materials, with very little pigments or minerals. They allow characterising properly the organic matter, whereas painting layers usually contain high concentrations of particles, in particular pigments. The chemical nature of these particles impacts the drying and ageing of paint film and thus affects its luminescence properties. Optical properties of the particles (absorption, scattering) also directly affect the measurement of the binding media luminescence, and thus need to be corrected.[68,69]

Synchrotron DUV/visible photoluminescence could therefore be inserted as an early step in the sequence of methods used to study a range of historical cross-sections. But recent work have also the asset of the technique for the study of comp[lex] materials in a diversity of research areas such osteoporosi[s] studies by discriminating osteocytes versus the bone matri[x] from amino acid composition,[70] and the study of microscale heterogeneities in metal oxides.[71,72] Here we show that complex organic-based structures, recognised as difficult to tackle, ca[n] be analysed and imaged with vastly improved contras[t] compared to conventional methods. In a wider sense, imagi[ng] the chemical speciation at the submicrometre scale to understand very fine organic structures and materia[l] distribution opens up new perspectives for fields such as biomedicine, xylology, forensics and polymer science.

Acknowledgements

We thank Balthazar Soulier for the preparation of the samp[le] from the Laux Maler lute and for his helpful comment[s] Camille Simon-Chane (Cité de la musique) for fruitf[ul] discussions, and Anne Forray-Carlier (Musée des Arts Décoratifs) for allowing the study of the Buchstetter mandora. Beamtime was funded by Synchrotron SOLEIL under proj[ect]s no. 20090761 and 20120487. The 'R' SpectroMicro package is developed by Serge Cohen (IPANEMA). The authors thank Dr Reynald Hurteaux and Horiba Europe Research Cent[re] (Palaiseau) for providing access to their Fluorolog 3 2-iHR32[0] instrument to perform PL spectroscopy measurements.

Notes and references

[a] *Equipe Conservation Recherche du Musée de la musique, CRC USR 3224, Cité de la musique, 221 avenue Jean Jaurès, F-75019 Paris, France. E-mail: jpechard@cite-musique.fr. Twitter: @echard_jp*
[b] *IPANEMA USR 3461, CNRS, ministère de la Culture et de la Communication, BP48 Saint-Aubin, F-91192 Gif-sur-Yvette, France. http://ipanema.cnrs.fr*
[c] *Scientific Research Department, National Gallery of Art, 4th and Constitution Avenue NW, Washington D.C. 20565, United States of America.*
[d] *Synchrotron SOLEIL, BP48 Saint-Aubin, F-91192 Gif-sur-Yvette, France.*

1 M. Thoury, J.-P. Echard, M. Réfrégiers, B. H. Berrie, A. Nevi[n], J. Jamme and L. Bertrand, *Anal. Chem.*, 2011, **83**, 1737-1745.
2 L. M. Condax, *Catgut Acoust. Soc. Newslett.*, 1982, 31-36.
3 C. Y. Barlow, P. P. Edwards, G. R. Millward, R. A. Raphael and D. J. Rubio, *Nature*, 1988, **332**, 313.
4 J.-P. Echard, in *Le violon italien - Une seconde voix humaine*, ed. F. Lainé, Opéra de Dijon - Aparté, Dijon, 2012, pp. 90-102.
5 S. F. Sacconi, in *I segreti di Stradivari*, Libreria del convegno, Cremona, 1972, pp. 159-191.
6 K. Padding, *J. Violin Soc. Amer. : VSA Papers*, 2007, **21**, 160-165.
7 B. Brandmair, S.-P. Greiner and J. Röhrmann, *Stradivari varnish : scientific analysis of his finishing technique on sele[ct] instruments*, Himmer AG, Augsbourg, 2010.
8 J.-P. Echard and B. Lavédrine, *J. Cult. Herit.*, 2008, **9**, 420-429.
9 V. Mazel, P. Richardin, D. Touboul, A. Brunelle, P. Walter and C. Laprévote, *Anal. Chim. Acta*, 2006, **570**, 34-40.
10 J. Sanyova, S. Ceroy, P. Richardin, O. Laprévote, P. Walter and A. Brunelle, *Anal. Chem.*, 2011, **83**, 753-760.
11 K. Keune and J. J. Boon, *Anal. Chem.*, 2004, **76**, 1374-1385.

12 M. R. Derrick, D. C. Stulik, J. M. Landry and S. P. Bouffard, *J. Am. Inst. Conserv.*, 1992, **31**, 225-236.

13 M. Cotte, J. Susini, V. A. Solé, Y. Taniguchi, J. Chillida, E. Checroun and P. Walter, *J. Anal. At. Spectrom.*, 2008, **23**, 820-828.

14 J.-P. Echard, M. Cotte, E. Dooryhee and L. Bertrand, *Appl. Phys. A*, 2008, **92**, 77-81.

15 E. Joseph, S. Prati, G. Sciutto, M. Ioele, P. Santopadre and R. Mazzeo, *Anal. Bioanal. Chem.*, 2010, **396**, 899-910.

16 G. Sciutto, P. Oliveri, S. Prati, M. Quaranta, S. Lanteri and R. Mazzeo, *Anal. Bioanal. Chem.*, 2013, **405**, 625-633.

17 A. Rizzo, *Anal. Bioanal. Chem.*, 2008, **392**, 47-55.

18 M. Spring, C. Ricci, D. A. Peggie and S. G. Kazarian, *Anal. Bioanal. Chem.*, 2008.

19 R. Mazzeo, E. Joseph, S. Prati and A. Millemaggi, *Anal. Chim. Acta*, 2007, **599**, 107-117.

20 J.-P. Echard, L. Bertrand, A. von Bohlen, A.-S. Le Hô, C. Paris, L. Bellot-Gurlet, B. Soulier, A. Lattuati-Derieux, S. Thao, L. Robinet, B. Lavédrine and S. Vaiedelich, *Angew. Chem. Int. Ed.*, 2010, **49**, 197-201.

21 L. Bertrand, L. Robinet, S. X. Cohen, C. Sandt, A.-S. Le Hô, B. Soulier, A. Lattuati-Derieux and J.-P. Echard, *Anal. Bioanal. Chem.*, 2011, **399**, 3025-3032.

22 B. Soulier, S. Zumbühl, J.-P. Echard, N. Scherrer and K. Wyss, *Z. Ksttech. & Konserv.*, 2012, **26**, 462-471.

23 G. Latour, J.-P. Echard, M. Didier and M.-C. Schanne-Klein, *Optics Express*, 2012, **20**, 24623-24635.

24 R. C. Wolbers and G. Landrey, Preprints of 15th Annual Meeting of American Institute for Conservation, Washington, D.C., 1987.

25 I. C. A. Sandu, S. Schäfer, D. Magrini, S. Bracci and C. A. Roque, *Microsc. Microanal.*, 2012, **18**, 860-875.

26 L. H. Oakley, S. A. Dinehart, S. A. Svoboda and K. L. Wustholz, *Anal. Chem.*, 2011, **83**, 3986–3989.

27 M. Thoury, M. Elias, J.-M. Frigerio and C. Barthou, *Appl. Spectrosc.*, 2007, **61**, 1275-1282.

28 L. S. Dolci, G. Sciutto, M. Guardigli, M. Rizzoli, S. Prati, R. Mazzeo and A. Roda, *Anal. Bioanal. Chem.*, 2008, **392**, 29-35.

29 G. Sciutto, L. Dolci, A. Buragina, S. Prati, M. Guardigli, R. Mazzeo and A. Roda, *Anal. Bioanal. Chem.*, 2011, **399**, 2889-2897.

30 A. Heginbotham, V. Millay and M. Quick, *J. Am. Inst. Conserv.*, 2006, **45**, 89-105.

31 J. Arslanoglu, J. Schultz, J. Loike and K. Petersen, *Journal of Biosciences*, 2010, **35**, 3-10.

32 J. Schultz and K. Petersen, Adhesives and Consolidants for Conservation, Ottawa, 2011.

33 L. Cartechini, M. Vagnini, M. Palmieri, L. Pitzurra, T. Mello, J. Mazurek and G. Chiari, *Acc. Chem. Res.*, 2010, **43**, 867-876.

34 G. A. Wagnières, W. M. Star and B. C. Wilson, *Photochem. Photobiol.*, 1998, **68**, 603-632.

35 J. R. Lakowicz, in *Principles of Fluorescence Spectroscopy*, Springer, New York, 3rd edn., 2006, pp. 529-575.

36 G. Bottiroli and A. G. Galassi, Scientific methodologies applied to works of art, Florence, Italy, 1984.

37 J.-P. Echard and L. Bertrand, *Spectrosc. Eur.*, 2010, **22**, 12-15.

38 A. Nevin, S. Cather, D. Anglos and C. Fotakis, *Anal. Chim. Acta*, 2006, **573-574**, 341-346.

39 A. Nevin, S. Cather, A. Burnstock and D. Anglos, *Appl. Spectrosc.*, 2008, **62**, 481-489.

40 A. Nevin, D. Comelli, G. Valentini, D. Anglos, A. Burnstock, S. Cather and R. Cubeddu, *Anal. Bioanal. Chem.*, 2007, **338**, 1897-1905.

41 A. Nevin, D. Anglos, S. Cather and A. Burnstock, *Appl. Phys. A*, 2008, **92**, 69-76.

42 A. Nevin, J.-P. Echard, M. Thoury, D. Comelli, G. Valentini and R. Cubeddu, *Talanta*, 2009, **80**, 286-293.

43 L. Bertrand, M. Thoury and E. Anheim, *J. Cult. Herit.*, 2013, **14**, 277-289.

44 F. Jamme, S. Kascakova, S. Villette, F. Allouche, S. Pallu, V. Rouam and M. Réfrégiers, *Biology of the Cell*, 2013.

45 V. Rouam, F. Jamme, A. Giuliani, B. Lagarde, S. Rey, J. P. Duval and M. Réfrégiers, *Journal of Physics: Conference Series*, 2013, **425**, 122005.

46 R Development Core Team, *R: A language and environment for statistical computing*, (2008) R Foundation for Statistical Computing, Vienna, Austria.

47 F. Jamme, S. Villette, A. Giuliani, V. Rouam, F. Wien, B. Lagarde and M. Réfrégiers, *Microsc. Microanal.*, 2010, **16**, 507-514.

48 J. Dugot, ed., *Les luths (Occident) - Catalogue des collections du Musée de la musique (vol. 1)*, Cité de la musique, Paris, 2006.

49 J.-P. Echard, Ph.D. thesis, Muséum National d'Histoire Naturelle, 2010.

50 J. Mallégol, L. Gonon, J. Lemaire and J.-L. Gardette, *Polymer Degradation and Stability*, 2001, **72**, 191-197.

51 E. R. de la Rie, *Stud. Conserv.*, 1982, **27**, 65-69.

52 J.-J. Wu and D. R. Eyre, *Biochem.*, 1984, **23**, 1850-1857.

53 D. R. Eyre, S. Apon, J.-J. Wu, L. H. Ericsson and K. A. Walsh, *FEBS Lett.*, 1987, **220**, 337-341.

54 D. R. Eyre, M. A. Paz and P. M. Gallop, *Annu. Rev. Biochem*, 1984, **53**, 717-748.

55 D. R. Eyre and J.-J. Wu, *Top. Curr. Chem.*, 2005, **247**, 207-229.

56 F. W. J. Teale and G. Weber, *Biochem. J*, 1957, **65**, 476-482.

57 A. Bairoch and R. Apweiler, *Nucleic Acids Res.*, 2000, **28**, 45-48.

58 F. W. J. Teale, *Biochem. J*, 1960, **76**, 381-388.

59 M. De Keghel, *Traité général de la fabrication des colles, des glutinants et matières d'apprêts*, Gauthier-Villars, Paris, 1959.

60 I. Vazquez-Coos and R. W. Meyer, *IAWA Journal*, 2008, **29**, 129-141.

61 V. de Micco and G. Aronne, *Biotech. Histochem.*, 2007, **82**, 209-216.

62 A. C. Wiedenhoeft, in *Wood Handbook, Wood as an Engineering Material*, Forest Products Laboratory, Madison, WI, 2010, pp. 1-18.

63 B. Albinsson, S. Li, K. Lundquist and R. Stomberg, *J. Mol. Struct.*, 1999, **508**, 19-27.

64 L. Bertrand, S. Schöder, D. Anglos, M. B. H. Breese, K. Janssens, M. Moini and A. Simon, *Trends in Analytical Chemistry*, 2014.

65 L. Bertrand, M. Cotte, M. Stampanoni, M. Thoury, F. Marone and S. Schoeder, *Physics Reports*, 2012, **519**, 21-96.

66 M. Cotte, E. Checroun, V. Mazel, V. A. Solé, P. Richardin, Y. Taniguchi, P. Walter and J. Susini, *e-PS*, 2009, **6**, 1-9.

67 A. Rizzo, N. Shibayama and D. P. Kirby, *Anal. Bioanal. Chem.*, 2011, **399**, 3093-3107.

68 G. Verri, C. Clementi, D. Comelli, S. Cather and F. Piqué, *Appl. Spectrosc.*, 2008, **62**, 1295-1302.

69 C. Clementi, C. Miliani, A. Romani, U. Santamaria, F. Morresi, M. K. and G. Favaro, *Spectrochim. Acta A*, 2009, **71**, 2057-2062.

70 S. Pallu, G. Y. Rochefort, C. Jaffre, M. Réfrégiers, D. B. Maurel, D. Benaitreau, E. Lespessailles, F. Jamme, C. Chappard and C.-L. Benhamou, *PLoS One*, 2012, **7**, e43930.

71 L. Bertrand, M. Réfrégiers, B. H. Berrie, J.-P. Echard and M. Thoury, *Analyst*, 2013, **16**, 4463-4469.

72 M. Thoury, M. Réfrégiers and L. Bertrand, *Microsc. Microanal*, 2014, **20**, 2022-2023.